Scanning Electron Microscopy

Volume 1985 | Number 3 Article 1

7-1-1985

Secondary Electron Imaging in the Scanning Transmission Electron Microscope

R. M. Allen
Sandia National Laboratories

SCANNING ELECTRON MICROSCOPY/1985/III (Pages 905-918)
SEM Inc., AMF O'Hare (Chicago), IL 60666-0507 USA

SECONDARY ELECTRON IMAGING IN THE SCANNING TRANSMISSION ELECTRON MICROSCOPE

R. M. Allen*

Sandia National Laboratories, Livermore, CA 94550

(Paper received March 24, 1984: manuscript received July 01, 1985)

Abstract

The detailed correlation of surface morphology and subsurface microstructure has been made possible by the scanning transmission electron microscope. This instrument provides the capability for simultaneous and independent secondary electron and transmitted electron imaging from the same sample area. This includes the ability to generate mixed secondary/transmitted electron images, which form a concise visual presentation of the information in the two component images.

Correlative surface and through-volume specimen examination of this type has most frequently been applied to backthinned samples, which are specifically prepared in a way which produces electron-transparent material in the immediate vicinity of a surface of interest on the original bulk sample. However, the technique has also been found to be useful for relating local microstructural features to the overall structure of the sample, and for determining the local specimen geometry for microanalysis by energy dispersive x-ray spectrometry. The formation of a mixed secondary/transmitted electron image also serves as a novel means of signal processing which reduces the difficulty of forming a transmitted image from regions adjacent to the edges of a thin foil sample.

KEY WORDS: Scanning transmission electron microscopy, secondary electron imaging, transmitted electron imaging, image mixing, image processing, backthinning, microanalysis, x-ray absorption, foil thickness, hole glare, image contrast.

*Address for correspondence:
Materials Development Division 8312
Sandia National Laboratories
Livermore, CA 94550
Phone No: (415) 422-2861

Introduction

Scanning transmission electron microscopes (STEM's) can be used to form images from a wide variety of the signals which emanate from samples under exposure to a high energy electron beam. For a typical instrument operated in its scanning mode, this would include images formed from transmitted electrons (possibly energy-filtered), secondary electrons, backscattered electrons, and diffracted electrons (using an annular dark field detector). In most modern STEM's these signals can be simultaneously and independently detected, electronically-processed, and displayed. This provides the opportunity to correlate the information contained in these different signals from the same sample area. This correlation may be accomplished either by simply comparing the images of interest, or by actually mixing these images together prior to display in an effort to obtain new information from the sample, or a more visually concise presentation of the originally available information. These possibilities have been discussed in detail in recent papers on image mixing (Jones and Smith, 1978, Isaacson et al., 1980).

One of the physically significant correlations of disparate information which may be accomplished in a STEM is the comparison of a secondary electron (SE) image of a sample region with the bright-field transmitted electron (TE) image from the same region. This comparison serves to relate the sample surface features (observed in the SE image) to the microstructure in the region immediately underlying the sample surface (observed in the through-volume TE image). The ability to correlate surface and subsurface structures through the use of a single instrument has led to work establishing the potential of the STEM as a tool for the understanding of the development of surface morphology during fracture, (De Vries and Mastenbroek, 1977, Katagiri et al., 1980, Nix and Flower, 1982), wear, (Carpenter, 1978, Carpenter et al., 1980), corrosion (Smith et al., 1979, Scamans and Tuck, 1979) and oxidation (Field et al, 1980), and the manufacture of semiconductor circuit devices (Anderson and Ramsey, 1979, Rackham and Steeds, 1980). Employing secondary electron imaging as an adjunct to transmitted electron imaging has also been found

to be quite helpful in the day-to-day use of a STEM for the examination and analysis of a wide variety of samples, as will be shown.

This paper will deal with secondary electron imaging in a STEM, with a particular focus on the utility of relating SE and TE information. The components and operation of a typical system which can be used to generate correlated SE and TE images from a STEM, including mixed SE/TE images, will be briefly described. This will be followed by examples of the application of secondary electron imaging to the examination of backthinned samples and samples obtained from heterogeneous specimens such as welds and alloy powder compacts. A discussion of the benefits of the technique as an aide during the STEM microanalysis and imaging of thin foils in general will also be included.

Correlated Secondary Electron/ Transmitted Electron Imaging

Instrumentation

The instrument used in the present work was a JEOL 200CX TEMSCAN equipped with a standard transmitted electron detector and secondary electron detector, a side-entry Si(Li) detector for energy-dispersive x-ray spectrometry (EDS), and a commercially-available analog signal mixing system. The two electron detectors are both scintillator/photomultiplier types. In this microscope, as is typical for a combination transmission electron microscope/STEM (TEM/STEM) (Williams and Edington, 1981a), the SE detector is seated above the objective lens pole piece out of the line of sight of the sample. The scintillator is biased to 10kV to attract the low energy secondary electrons which spiral back up through the objective lens. This bias is not shielded by a Faraday cage as it is in a conventional SEM, and as a result a noticeable shift in the TE scanning image occurs when the SE detector high-voltage is turned off or on. As a result, the voltage on this detector must be left on if correlated TE/SE imaging is to be done, particularly at high magnifications. At this position in the column, the secondary electron detector forms images from the top (probe-entry) surface of a sample held in the side-entry goniometer stage. With the sample tilted for EDS analysis, this is the same surface which faces the EDS detector. The transmitted electron detector is located below the TEM camera chamber at some distance beneath the sample.

A block diagram of the relevant portions of the signal mixing system is shown in Fig. 1. Signals from the dedicated amplifiers serving the TE and SE detectors are first passed into an image selector box and the "channel 1" and "channel 2" outputs chosen. The two outputs are fed into the signal mixer, which allows control over the polarity of the input signals, the type of mixing (i.e., addition or division) which will be performed, and the relative balance between the two input signals in the final mix. The balance control is continuously adjustable from 100% channel 1/ 0% channel 2 to 0% channel 1/ 100% channel 2. The output from the mixer is passed through another amplifier, and then serves as one input to a split screen display device. The second input to the split screen device is the original unmixed channel 2 signal. The output from the split screen device is viewed on a waveform monitor and a cathode ray tube (CRT) display. Images are recorded on a second CRT with 200 line/cm resolution. A description of the internal operation of analog signal mixers may be found elsewhere (Isaacson et al., 1980). For the remainder of this paper, the discussion will be limited to the processing and applications of normal polarity images only. Several examples of the mixing of SE and TE images of both normal and reverse polarity (for biological samples) can be found elsewhere (Kokubo et al., 1980, Hosoi et al., 1981).

Assuming, for the moment, that the secondary electron signal is chosen for channel 1, and the transmitted electron signal chosen for channel 2, then the system shown in Fig. 1 can yield the following full-screen displays: SE image, TE image, and mixed SE/TE image. In addition, it is also possible to form a split-screen display with a mixed SE/TE image on one side of the screen and an unmixed TE image on the other side. With this system, the mixed image may be varied considerably (by using the amplifier for the channel 1 signal, the balance control, and the post-mixing amplifier controls) without significantly changing the unmixed reference image. An example of this capability is shown in Fig. 2, where a consecutive series of split screen images was made by changing the balance, gain, and level of the mix in the left halves of the images while the right halves show the fixed TE reference image

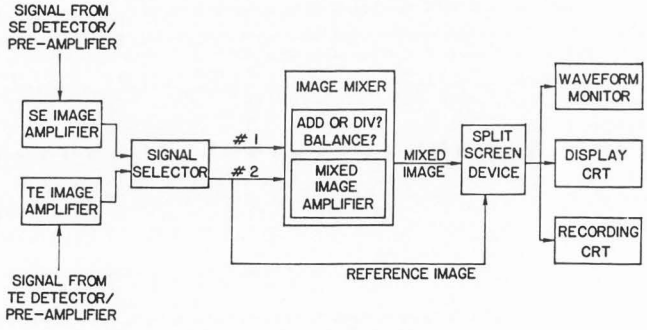

Fig. 1: Block diagram of signal mixing and display system.

Fig. 2: Illustration of the use of a fixed reference image during image mixing. The left hand side of each photograph is a mixed SE/TE image of the sample region; the relative proportion of each component in the mix is indicated at the top as %SE vs. %TE signal. The right hand side is a fixed TE reference image from the same sample area. It can be seen that the mixed image can be varied widely (i.e., from 100% SE/0% TE to 0% SE/100% TE) without changing the reference image. The sample is an electropolished thin foil of a high-alloy stainless steel; Cr carbide particles are visible along the grain boundaries, Ti carbide particles can be seen in the matrix.

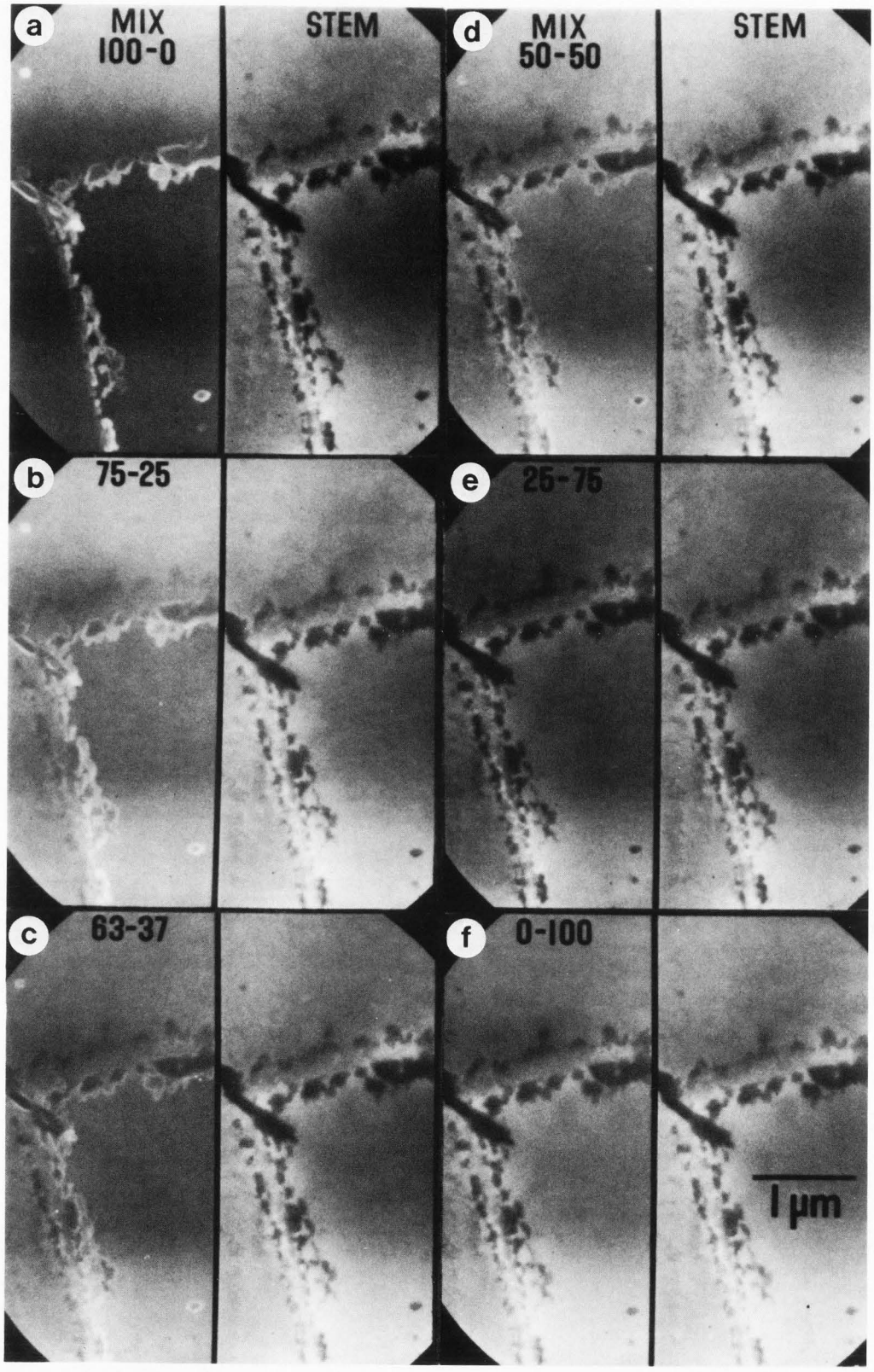
a
MIX
100-0
STEM
d
MIX
50-50
STEM
b
75-25
e
25-75
c
63-37
f
0-100
1 µm

throughout. This latter mode was wired-in at the suggestion of this author to provide a reference image against which the quality of the mixed image may be directly compared.

Imaging Conditions

Procedures for optimizing TE and SE images, including such things as alignment, choice of beam current, lens settings, and specimen tilt, and the use of various apertures, are described elsewhere (see, for example, Goldstein, 1975, Newbury, 1975, Humphreys, 1979, Williams and Edington, 1981b, and Williams, 1982). It should be realized that, when trying to correlate these images in a STEM, some choices for operating conditions involve trade-offs. For instance, the SE signal and contrast from a sample increase markedly if the sample surface is tilted away from the horizontal (Newbury, 1975). On the other hand, tilting the sample through large angles also increases the effective thickness of a thin foil, reducing the extent of the area transparent to the electron beam, and making TE imaging more difficult. As a second example of a trade-off, use of a smaller condenser aperture reduces the convergence angle of the electron probe, improving the contrast in a TE image (Humphreys, 1979), as well as increasing the depth of field of the SE image when dealing with a sample with an irregular surface (Goldstein, 1975). This improvement in image contrast offsets to some extent the effect on the TE image of the reduction in probe current accompanying the use of the smaller aperture. The smaller probe current will have a more deleterious effect on the signal-to-noise ratio of the SE image, however, particularly for relatively smooth foils, since the contrast in this image depends primarily on the topography of the foil surface rather than on diffraction effects as in the TE image. The choices in any given situation obviously depend on the nature of the foil being examined, and on the information desired in the final image.

Once the imaging conditions are chosen, the SE and TE images can be assigned to the two different display channels. By turning the balance control from one stop to the other the two component images can be observed. This allows the two images to be individually optimized with the controls of their respective dedicated amplifiers. The average signal levels are made approximately the same, and this is checked with the wave-form monitor. With the two components set, turning the balance control slowly between the stops appears to "fade" one image into the other, making visual comparison of the SE and TE images extremely simple. Alternatively, if a mixed SE/TE image is desired, the balance control is set depending on the relationship which is to be expressed between the surface and subsurface microstructure in the final image. The contrast and brightness levels for the mixed image are adjusted by the use of the controls for the amplifier dedicated to the mixed image itself.

Applications of Secondary Electron Imaging

Backthinned Samples

The sample preparation technique known as backthinning is often employed to produce thin foils specifically for correlating surface features to the microstructure underlying the surface. Backthinned samples are prepared from bulk samples as follows (Goodhew, 1972). The surface of interest is first sliced off the starting sample. The slice is then typically spark-cut to yield a group of 3 mm diameter disks, each of which has a portion of the original surface of interest on one of its sides. This side is coated with a lacquer for protection during subsequent handling, and then the disk is thinned to electron transparency by electropolishing or ion-milling the material from the opposite (the "back") side. After thinning the protective lacquer is removed with the appropriate solvent and the sample can be examined in the microscope. The sample will have a portion of the original surface of interest on one of its sides and, assuming little or no leakage of electrolyte under the lacquer occurred during sample perforation, this surface topography should extend up to the edge of the hole in the foil. The electron transparent areas in the sample will be representative of the microstructure in the material in the region immediately underlying the surface of interest. The original application of backthinning as a sample preparation technique was by Hirsch et al., 1959, who used it to examine, in a conventional transmission electron microscope (CTEM), the dislocation structure below slip steps on the surfaces of deformed samples of an 18-8 stainless steel.

It is the STEM, however, which appears to be ideally suited for samples made in this fashion, with its potential for correlative SE (surface) and TE (through-volume) imaging. An example of this is shown in Figs. 3-5. A backthinned sample was prepared from a fracture surface on a sample of a manganese-modified 316 stainless steel. A low magnification SE image of this sample may be seen in Fig. 3, which shows the region of the fracture surface in the vicinity of the hole developed during jet polishing from the back side. Figure 4 shows the SE, TE, and mixed TE/SE images which were taken of a portion of the sample area near the hole. The TE image in Fig. 4a indicates that a patch of thin area was produced in the sample away from the edge of the hole. By itself, however, the information in the TE image does not reveal anything about any feature on the fracture surface which might be associated with the thin area. The SE image (Fig. 4b) from the same area taken at the same sample tilt, shows a dimple to be present on the fracture surface at this location. The mixed image in Fig. 4c proves that the fine dislocation cell structure visible in the TE image underlies the bottom wall of the dimple visible in the SE image. Further, the boundaries of the thin patch are in part determined by the steep side walls of the dimple. Having the ability to directly correlate the surface and through-volume images from a backthinned sample in a STEM greatly increases the information which can be obtained from the sample.

Figure 5 shows a higher magnification mixed image of this same area. This mixed image provides a concise visual correlation between the two distinctly different component images, which leaves no doubt as to how the two images relate.

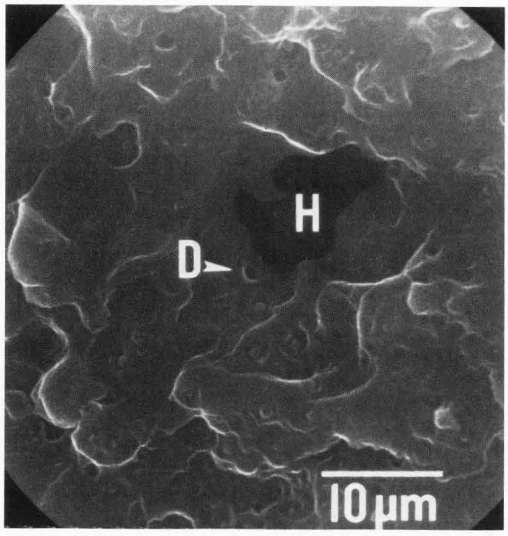

Fig. 3: Low magnification SE image of backthinned fracture surface sample in manganese-modified 316 stainless steel. The hole in the sample produced during thinning has been marked at H. D shows the location of the dimple examined at higher magnifications in Figs. 4 and 5.

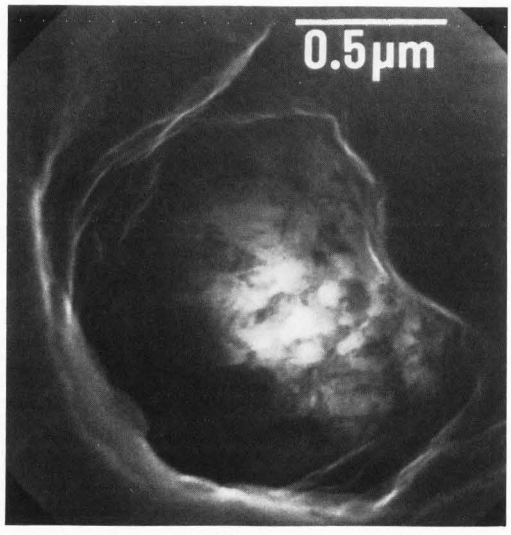

Fig. 5: Higher-magnification mixed TE/SE image taken of dimple in backthinned fracture surface sample.

In addition, for a backthinned sample the two components often contain complementary image information. The TE information comes from the thinner, transparent, regions of the film, which do not yield much information in the SE image compared to the non-transparent areas where the sample thickness varies widely. As a result, the two image components together tend to "fill up" a field of view rather efficiently in a mixed image.

Many examples of STEM studies using comparative SE and TE images on backthinned samples have

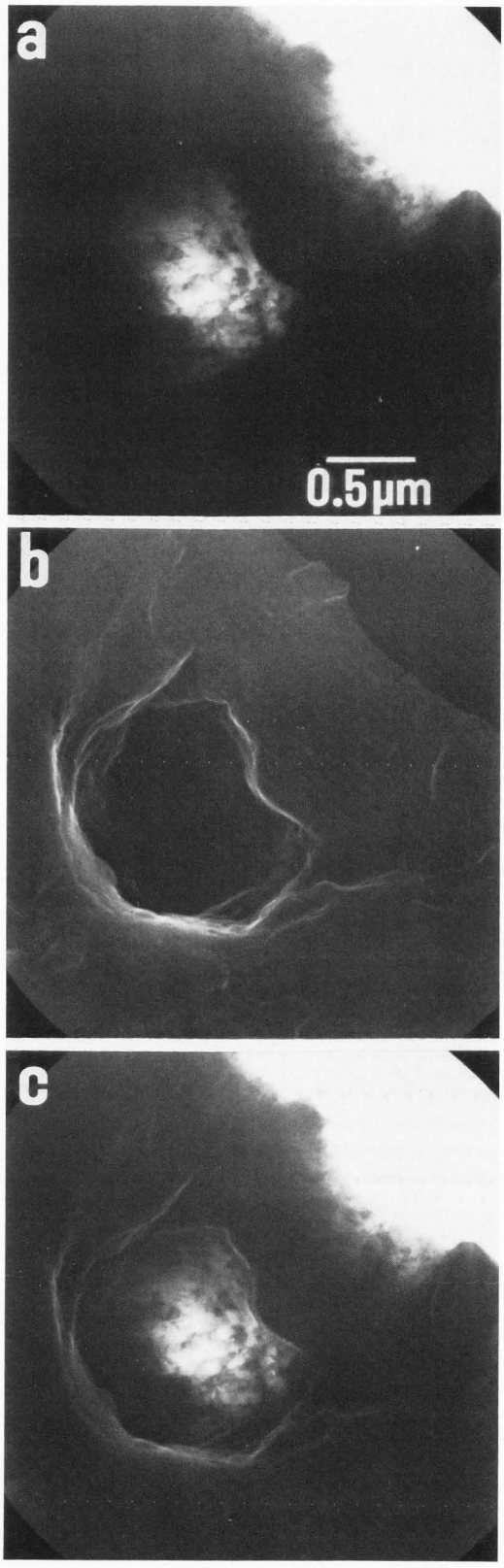

Fig. 4: Images of region marked D in Fig. 3. a) TE image. b) SE image. c) Mixed TE/SE image.

been reported in the literature. Backthinned samples made from fatigue fracture surfaces in 304 stainless steel (De Vries and Mastenbroek, 1977), copper and brass (Katagiri et al., 1980), and 7010 aluminum alloy (Nix and Flower, 1982) have been examined in an attempt to relate fatigue striations on the fracture surfaces to the underlying dislocation structure. Backthinned samples have been prepared from 1100 aluminum and Cu-8%Al samples with wear tracks on their surfaces, and examined in STEM to relate the track morphology to underlying dislocation structure and local changes in grain structure (Carpenter, 1978, Carpenter et al., 1980). The corrosion of an Al-4%Cu alloy was studied using backthinned samples in a STEM, and it was found that the surface corrosion product formed first on Al_2Cu particles in the material, rather than at grain boundaries or on regions with high dislocation density (Smith et al., 1979). The effect of small Be additions on the prevention of oxidation in an Al-5%Mg alloy has also been investigated using backthinned samples in a STEM (Field et al., 1980); this study concentrated on the structure of the oxide films which form at the surface of the alloy. (Related work by Scamans and Tuck, 1979, has also been done using thin film corrosion samples to study the initial stages of hydrous oxide formation on various aluminum alloys.) Multilayer laser target materials have been characterized in a similar manner, by thinning from the back up to the target surface (Johnson et al, 1983).

Semiconductor circuit devices have also been a popular subject for investigation in the STEM. Such samples are backthinned from the substrate side to allow examination of the devices at the chip surface. This approach has allowed the comparative SE and TE imaging of embedded stainless steel impurity particles in silicon transistors (Anderson and Ramsey, 1979), and of the growth structures of several types of vapor-deposited metal/semiconductor contacts (Rackham and Steeds, 1980, Loveluck et al., 1977).

Heterogeneous Samples

An important question which arises when electron-transparent samples must be thinned from bulk starting specimens concerns the accuracy with which the structure in the tiny amount of thin area produced during sample preparation represents the actual structure in the bulk sample. This is a particularly crucial issue when dealing with notoriously inhomogeneous samples such as weldments and compacted alloy powders. Fortunately, multi-phase samples often show surface relief after thinning. This means that secondary electron images in the STEM can be used to locate the thin area within the overall sample, and so relate the local microstructure observed in transmission to the remainder of the bulk.

A simple example of this, found in the literature, deals with the STEM examination of thinned samples made from Ni-based superalloy powder particles held together by electroplated Ni (Field and Fraser, 1978). The objects of interest in these specimens were the 100 micrometer - diameter powder particles. Secondary electron imaging clearly revealed the locations of the particles, as well as how the thin area (produced by electropolishing) was distributed in and among them. Utilizing this SE imaging capability in the STEM conveniently avoided the possibility of straying out into an electroplated Ni region during subsequent TE imaging or microanalysis of the thin area.

Correlating the SE and TE images from a complex sample also aids in the interpretation of the local microstructure. An example is shown in Fig. 6. The material in question is explosively-compacted Al-6wt.%Si alloy powder. Previous microprobe investigation of this material showed it to be made up of basically four types of distinguishable microstructures: cellular powder particle remnants which appeared to survive the compaction process relatively unchanged; fine-grained rapidly-quenched splat-caps on the surfaces of some of these remnants which also survived the compaction process; cellular particle regions which were severely deformed during compaction; and fine-grained interparticle regions which may have melted and re-solidified during compaction.

This diverse microstructure is quite difficult to interpret when viewed in a transmitted electron image (see Fig. 6a). However, forming a secondary electron image of the surface of the thin area (Fig. 6b) clearly reveals the prior particle boundaries. In addition, the electropolishing solution used preferentially etches the Si-rich eutectic phase present along some of the cell boundaries in the structure. This additional information helps to assign the structure visible in the thinned region in a TE image to the general categories developed by lower magnification observation in the electron microprobe. Mixing a small proportion of the SE image directly into the TE image (Fig. 6c) proved to be a convenient means of correlating the two images and avoiding any question of where the prior particle boundaries were amidst the fine-celled structure of the material. This latter point was occasionally difficult to judge just from a side-by-side comparison of the SE and TE images alone.

A somewhat related example of the use of secondary electron images to aid in the interpretation of complex microstructures via STEM was reported in a study of high-stress contact fatigue in ball-bearings (Osterlund and Vingsbo, 1978). Thin foils, which consisted of complex mixtures of martensite, heavily deformed ferrite, and various carbides, were prepared from the bearings and then etched in Nital for 10 seconds to enhance their surface topography. Subsequent correlation of the SE image of the etched surface of the thin area with the TE image of its internal structure aided the identification of the phases present at a given region of the thin foil.

Secondary Electron Imaging as an Aid to STEM Microanalysis

Setting the Overall Sample Orientation for Microanalysis. It has been demonstrated that the geometrical relationship between the sample, EDS detector, and incident electron probe can significantly influence the results of the STEM microanalysis of a sample (Glitz et al., 1981, Zaluzec, 1981, Williams and Goldstein, 1981). This geometry should be set up so as to minimize possible absorption effects, particularly when

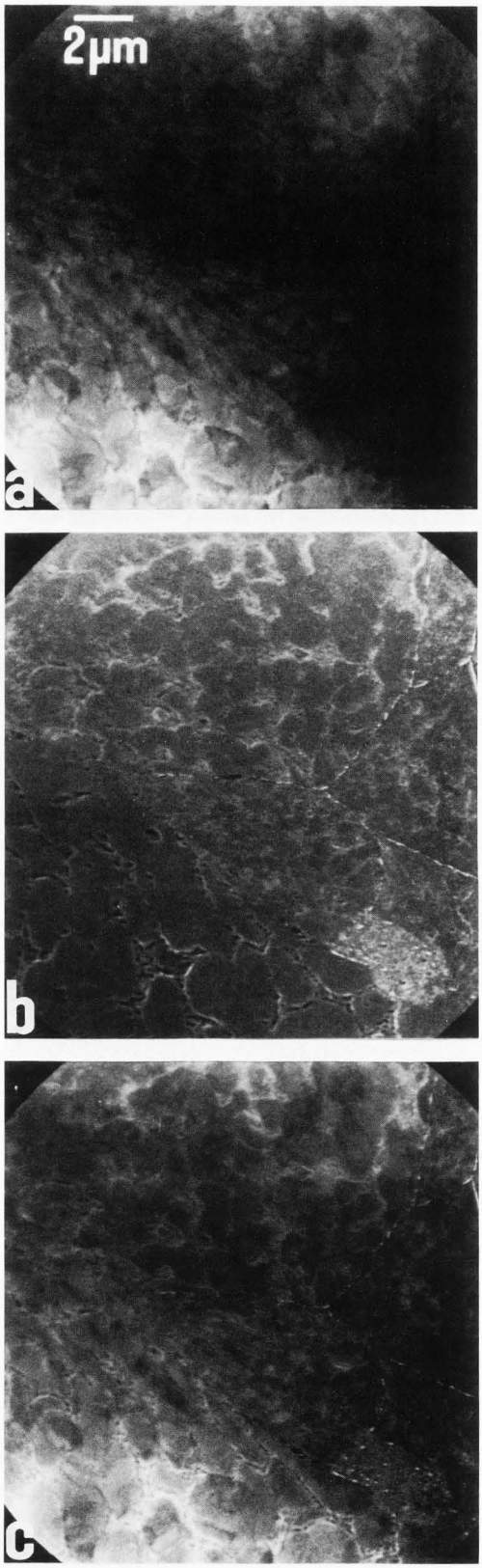

Fig. 6: Micrographs of region of dynamically-compacted Al-6%Si powder sample. a) TE image. b) SE image. Note the ease with which the individual prior particles can be identified. c) Mixed TE/SE image. The mix has been performed to allow the SE component to outline the prior particle boundaries in the TE image.

the Cliff-Lorimer thin-film approximation (Cliff and Lorimer, 1972; 1975) is to be used to analyze the EDS data. For example, assume that a thin foil has been prepared from a bulk sample for the purpose of measuring the concentration profiles of the alloying elements across the grain or cell boundaries present in the material. If the final thinning technique involved perforating a disk-shaped sample by jet-electropolishing or ion-milling, a roughly wedge-shaped cross-section will have been generated in the foil near the hole. The boundaries which should be analyzed in the thin foil are those which run perpendicular to the edge of the foil, because an analysis which runs parallel to the edge (perpendicular to these boundaries) would be performed with roughly constant foil thickness throughout (along an iso-thickness contour of the wedge). In addition, the sample should be positioned in the specimen holder so that the boundaries to be profiled are near the edge of the thin foil furthest from the EDS detector. This minimizes the path length for x-ray absorption in a wedge-shaped sample, and allows the x-rays escaping to the detector to travel in what are hopefully iso-concentration planes parallel to the boundaries being analyzed.

The proper geometry can be easily arranged using the SE imaging capability of a STEM. This is illustrated in Fig. 7 for a weld fusion zone sample cut from a bulk specimen of an Al-Cu alloy in a direction parallel to the local solidification cells. A very low magnification SE image such as the one shown in Fig. 7a includes a portion of the specimen holder in the field of view. Most holders designed for microanalysis will have a notch (for x-ray escape) or some other distinguishing characteristic which serves to show, in a low magnification image, the direction in which the EDS detector lies relative to the sample. For convenience, in the present case the scan direction has been rotated, using the SE image as a guide, to place the EDS detector off of the top edge of the image in Fig. 7a. A somewhat higher magnification SE image, Fig. 7b, taken with this same rotation, shows that the overall direction of the solidification cells will not meet the criteria recommended above. The cells which run perpendicular to the edge of the hole in the sample are located on the lower left or upper right in the image. To limit absorption effects the sample should be removed from the microscope and rotated to bring one set of these cells to the bottom of the image, opposite the detector.

Determining the Local Sample Geometry. At higher magnifications, secondary electron imaging can also aid STEM microanalysis by locating those features optimally positioned for analysis. For example, consider the effect of specimen geometry on the analysis of second phase particles in a thin foil. Figure 8 illustrates the problem. If

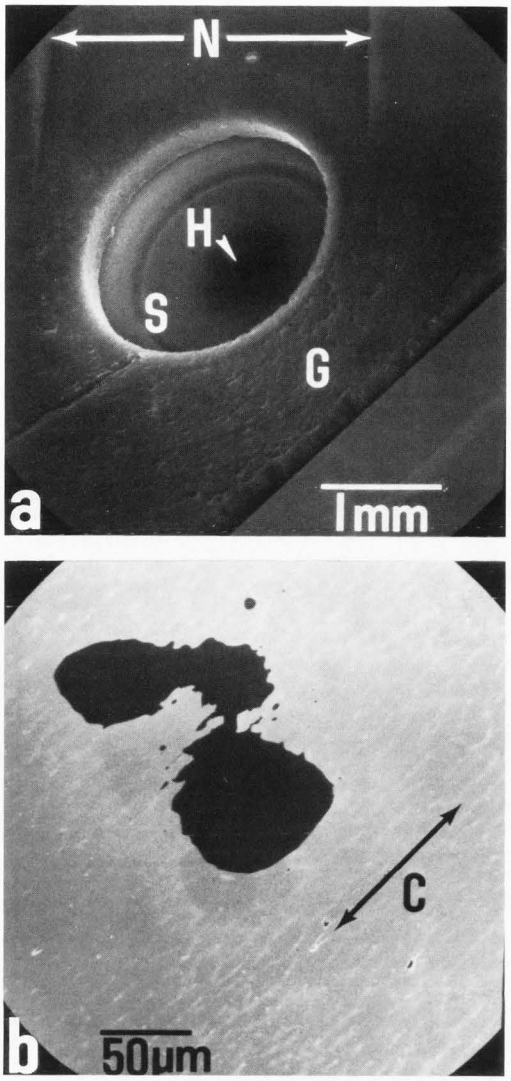

Fig. 7: Low magnification SE images of an Al-Cu weld sample in a graphite specimen holder. a) Very low magnification view to establish detector position relative to sample. The notch N in the graphite holder G points toward the detector; the scan direction has been rotated to bring this direction to the top of the display, for convenience. The sample can be seen at S; the hole in the sample, produced during thinning, is at H. b) Higher magnification SE image of the region of the sample around the hole. The direction of the solidification cells is shown at C. It can be seen that the cells run perpendicular to the edge of the hole along the lower left and upper right edges of the hole. Proper orientation of this sample for x-ray microanalysis would require rotating the sample within the holder to bring one of these edges to the bottom of the field of view.

an inclusion located below the surface of the sample facing the incident beam and x-ray detector is analyzed (Fig. 8a), probe spreading and

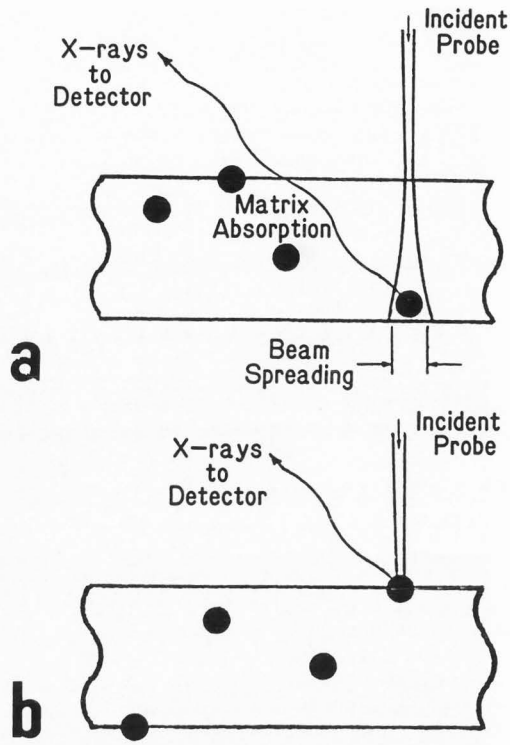

Fig. 8: Schematic illustration of possible sample geometries for the STEM analysis of second phase particles in a thin foil (taken from Allen, 1982). a) Analysis of a particle near the bottom surface of the foil. The characteristic x-ray signal from the particle may be reduced and distorted by spreading of the incident probe and x-ray absorption in the matrix above the particle. b) Analysis of a particle at the top surface of the foil, facing the incident probe and EDS detector. The particle sees the full probe current and the x-rays generated travel directly to the EDS detector without passing through intervening matrix material.

absorption of the particle's characteristic x-rays by the matrix will act to reduce and distort the signal generated by the particle. A much more favorable geometry for analysis is to have the inclusion actually on the surface of the sample facing beam and detector (Fig. 8b). In this case, the full probe current will hit the particle, maximizing its x-ray signal, and the x-rays will travel straight to the detector without passing through intervening matrix material, thereby minimizing absorption effects. As mentioned earlier, because the different phases in a multiphase sample tend to polish at different rates during sample preparation, second phases at the sample surface will often show relief in an SE image. Therefore, if the secondary electron detector in the STEM is located on the beam-entry/EDS detector side of the sample an SE image can easily be used to find inclusions at the sample surface which are optimally positioned for STEM analysis.

These considerations were demonstrated in an

experiment performed by this author on a thin foil made from a high-alloy stainless steel containing (Ti,Nb)C inclusions (Allen, 1982). Figure 9 shows the sample region analyzed in that study. Figures 9a-c are TE, SE, and mixed TE/SE micrographs which were taken of the sample as it was first put into the STEM. Figures 9d-f are similar micrographs which were taken after the sample was removed from the STEM, turned over, and then reinserted in the instrument. A comparison of the two TE images shows the left-right inversion of the sample structure which was a manifestation of the repositioning done to the sample. The two SE images clearly show the locations of the second phase particles which were on what were originally the top (Fig. 9b) and bottom (Fig. 9e) surfaces of the foil in this region. The mixed SE/TE images helped to unambiguously correlate the information in their two component images; as can be seen, the secondary electron component served to highlight the particles at the foil surface in each view.

With the information obtained from the SE images, a series of analyses were performed on a group of particles (numbered 1-7 in Fig. 9c) which were on one of the surfaces of the foil. Basically, a comparison was made between the x-ray spectrum obtained from each particle when it was down on the bottom foil surface (facing away from the incident beam and EDS detector), and from when it was up on the top foil surface (facing the beam and detector). One such comparison (for the particle numbered 2 in Fig. 9c) is shown in Figs. 10a and 10b. It can be seen that the niobium L-line and titanium K-line signals from the particle were significantly stronger when the particle was up on the top surface of the foil. For example, the measured Ti K-alpha intensity with the particle on the bottom foil surface was only 40% of the top surface value. A similar marked improvement in the measured particle x-ray signal was found for the other particles as well when they were in their optimum analysis positions on the top foil surface. Calculations were performed to show that the differences between the "top surface" and "bottom surface" spectra could be accounted for by the expected beam broadening and x-ray absorption effects illustrated in Fig. 8. It was pointed out that this effect of particle height would be especially important when dealing with light element analysis, where the soft x-rays generated would be strongly absorbed by most matrix materials.

The information on specimen geometry determined from the set of micrographs in Fig. 9 serves to locate markers (particles) on the top and bottom surfaces of the sample which may be used in making parallax-effect measurements of local foil thickness. For example, measurements made using the particles numbered 1, 2, B1, and B2 in Fig. 9 showed that the local foil thickness was 460 $\pm$ 25 nm. The method is similar to those suggested elsewhere, but the use of the SE signal to locate markers built in to the foil surfaces obviates the need for either stereomicroscopic observation to determine reference particles (Nankivell, 1962b), or the use of vapor deposition (Nankivell, 1962a) or latex spheres (von Heimendahl and Willig, 1980) to mark the sample surfaces. In common with other parallax techniques, including contamination spot separation measurements (Lorimer et al., 1976), reasonable estimates can be obtained for the height of objects totally within the foil as well.

Secondary electron imaging can also aid in the STEM analysis of thin foils by detecting surface artifacts associated with specimen preparation. For example, if any doubt exists as to whether or not some particles observed may be real or artifactual, a set of images such as those in Fig.9 can quickly establish the presence or absence of the particles in the foil interior. (In Fig.9 itself, the particle marked M in Fig. 9c does not show SE contrast in either foil orientation and therefore is clearly in the foil interior.) In addition, the SE image may reveal preferential etching at grain or cell boundaries. The local change in sample thickness at the boundary may then have to be taken into account when interpreting data taken during concentration profiling across such boundaries. Secondary electron imaging in the STEM has also been used to examine the buildup of contamination on sample surfaces during STEM analysis (Hren, 1979).

Finally, SE imaging can be of use on particulate samples as well. For STEM analysis, such samples are usually deposited in some fashion on a thin support film held on a transmission electron microscope grid. It again becomes necessary to consider the local geometry of the specimen in order to obtain accurate analyses. Figure 11 illustrates this point. The sample is powdered coal which has been dispersed on a holey carbon film held on a copper grid. Particles are present on both sides of the support film. The TE image of a region of this sample is shown in Fig. 11a. In order to avoid any effects of absorption, particle-particle screening, or overlap, the SE image was used to select only those particles for analysis which were on the top surface of the support film and had clear paths toward the EDS detector. As seen in Fig. 11b, the pure SE image of the area, this selection was easily done since the bottom surface particles visible in the TE image were invisible in the SE image. By mixing the SE and TE images together (see Fig. 11c), large areas of the support film could be quickly searched for appropriate particles for analysis. The utility of SE imaging in the STEM in regard to examining particulate samples has been commented on previously (Porter et al., 1979, Porter et al., 1982, McConville, 1983).

Mixed Secondary Electron/Transmitted Electron Imaging as a Means of Image Processing

A constant source of annoyance during the bright-field transmitted electron imaging of thin samples is the problem of "hole glare", i.e., the fact that in a TE image, if the hole in the specimen is in the field of view it will be the brightest object in the image. This generally sets the limit on the amount of contrast which can be achieved from the adjacent specimen region in a recorded image. However, in a secondary electron image, the hole is always the darkest object in the field of view, for the simple reason that no secondary electrons are generated there. In a mixed TE/SE image, therefore, these two extremes will tend to balance each other out,

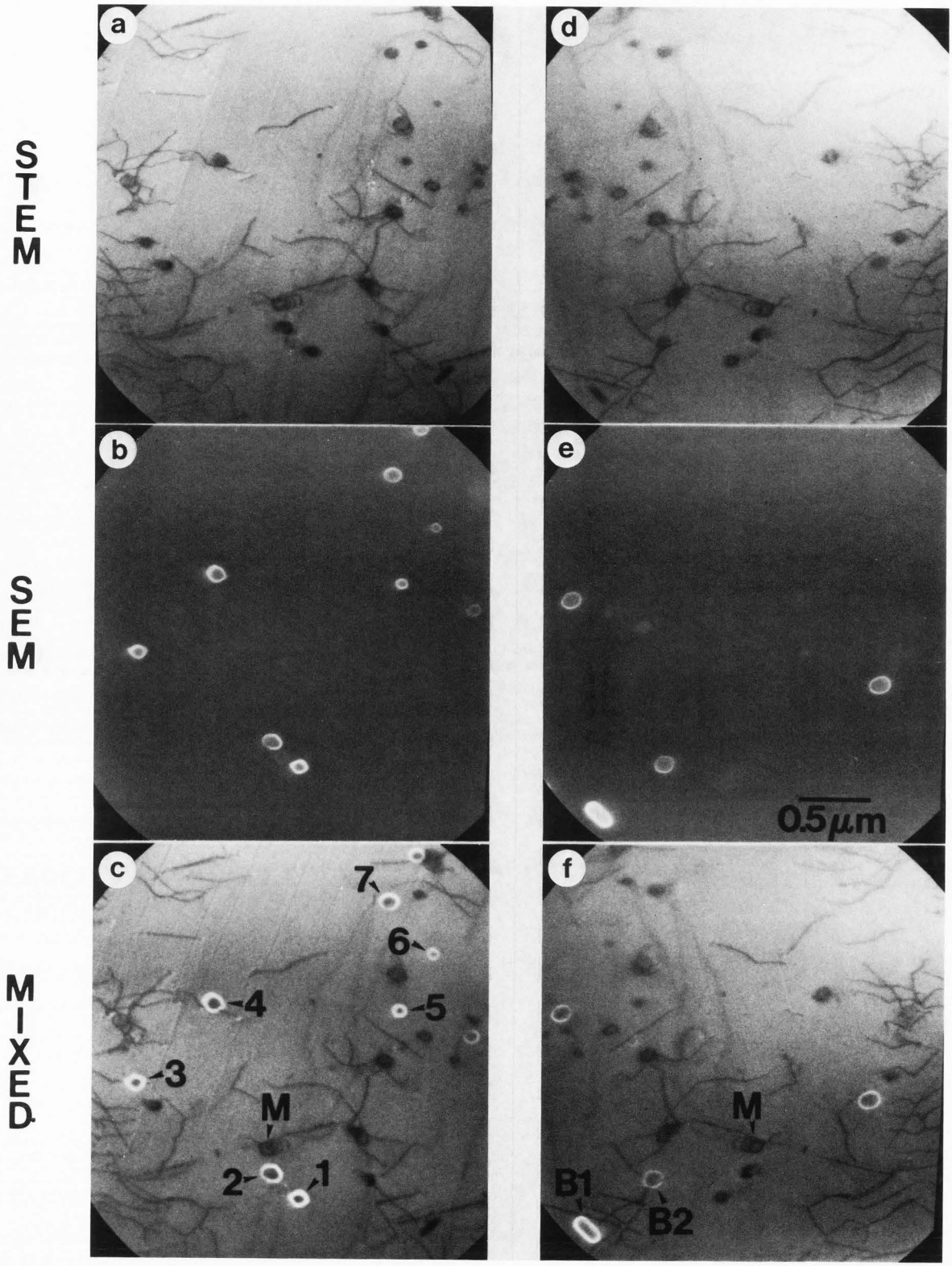
STEM
SEM
MIXED
a
b
c
d
e
f
0.5μm
7
6
5
4
3
M
2
1
M
B1
B2
Top Surface
Bottom Surface

Fig. 9

Fig. 9: Images of an electropolished thin foil of Alloy 800 (from Allen, 1982). The precipitates in the field of view are (Ti,Nb)C type. a-c) TE, SE, and mixed TE/SE images of a region of the sample. As can be seen in the mixed image, the SE component reveals the particles at the top surface of the foil in this view (e.g., the particles marked 1-7 in c)). d-f) TE, SE, and mixed TE/SE images of the same region of the sample after the foil was turned over. As can be seen from f), a new group of particles (e.g., B1 and B2) are now on the upper foil surface. Particle M does not show SE contrast in either of the foil orientations, and so must lie entirely within the foil. ←

and the hole will appear grayish. This provides the opportunity to increase the contrast of the image of the sample areas adjacent to the hole.

Figure 12 illustrates this assertion. Figure 12a is a standard TE image of the edge of a thin foil prepared from dynamically-compacted Al-6%Si powder alloy. Figure 12b is a mixed TE/SE image taken of this same sample area with the same overall range of contrast, as measured by the waveform monitor. It can be seen that the hole is no longer the brightest object in the image, as it is in Fig. 12a, and that the image of the sample appears much improved near the edge of the hole. This indicates that mixing SE and TE images together in the STEM may help to overcome the problem of hole glare and serve as an alternative option for signal processing to improve the appearance of TE images.

Conclusions

1. A STEM provides a unique opportunity to correlate information on a sample's surface morphology with information on the internal structure of the sample in the region immediately underlying the surface. This can be done because it is possible to independently form a secondary electron (surface) and transmitted electron (through-volume) image of the same sample area at the same time. Further, it is possible to mix these two images together to present this direct correlation in a visually concise, unambiguous manner.

2. Secondary electron imaging in a STEM finds applications in:

a) the examination of backthinned samples, as a means of correlating the desired surface and subsurface microstructural information,

b) the examination of heterogeneous samples, such as welds or alloy powder compacts, to aid in relating the local microstructure observed in the transmitted electron images to the overall structure of the sample,

c) day-to-day STEM microanalysis, where secondary electron imaging can determine information about sample geometry important for developing satisfactory microanalysis results, and avoiding misleading specimen preparation artifacts, and

d) the imaging of sample regions near the edge of thin foils, where the secondary electron component in a mixed secondary electron/transmitted electron image improves image quality by reducing the brightness of the hole image.

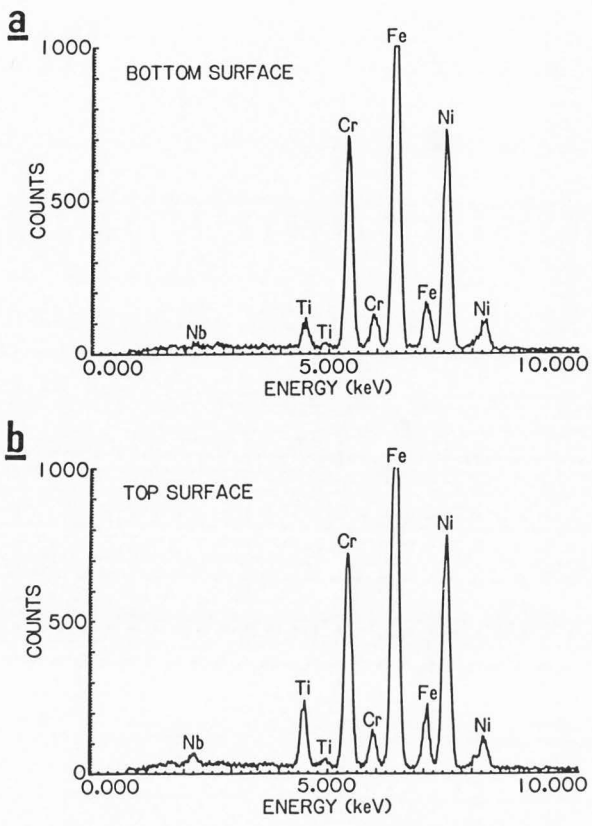

Fig. 10: EDS spectra taken from the particle numbered 2 in Fig. 9c. a) Spectrum with particle on bottom foil surface. b) Spectrum with particle on top foil surface. Note the improvement in the particle-related signal (i.e., the Nb and Ti signals) found in b). (From Allen, 1982.)

Acknowledgments

The author would like to thank Mr. Steven Orth and Mr. Donald Lind for preparing the various samples used as illustrative examples in this paper. This work was supported by the U.S. Department of Energy, DOE, under contract number DE-AC04-76DP00789.

References

Allen RM. (1982). Secondary Electron Imaging as an Aid to STEM Microanalysis. Ultramicroscopy 10, 237-245.

Anderson R, Ramsey JN. (1979). The Strategy of Analysis, in: Introduction to Analytical Electron Microscopy, J.J. Hren, J.I. Goldstein, D.C. Joy (eds), Plenum Press, New York, 575-593.

Carpenter RW. (1978). Application of an Analytical Electron Microscope to Surface Deformation and Wear Research, in: Electron Microscopy 1978, vol. 1, J.M. Sturgess (ed), Microscopical Society of Canada, Toronto, 588-589.

Carpenter RW, Wert JJ, Caldwell SG. (1980). Metal Surface Deformation and Subsurface Defect Structure: A Microscopy Correlation Study, in: Proceedings of the 38th Annual Meeting of the EMSA,

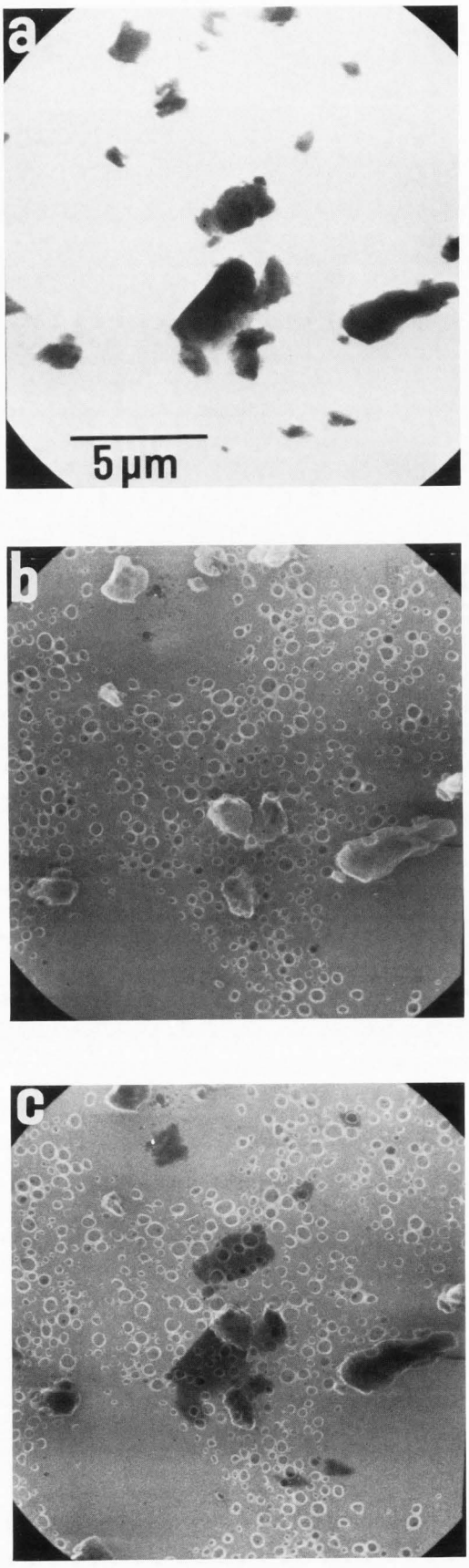

Fig. 11: a) TE, b) SE, and c) mixed TE/SE image of the same region of a sample of powdered coal. The powder particles were held on a holey carbon support film. Notice that particles clinging to the surface of the support film facing away from the SE detector are not visible in the SE component.

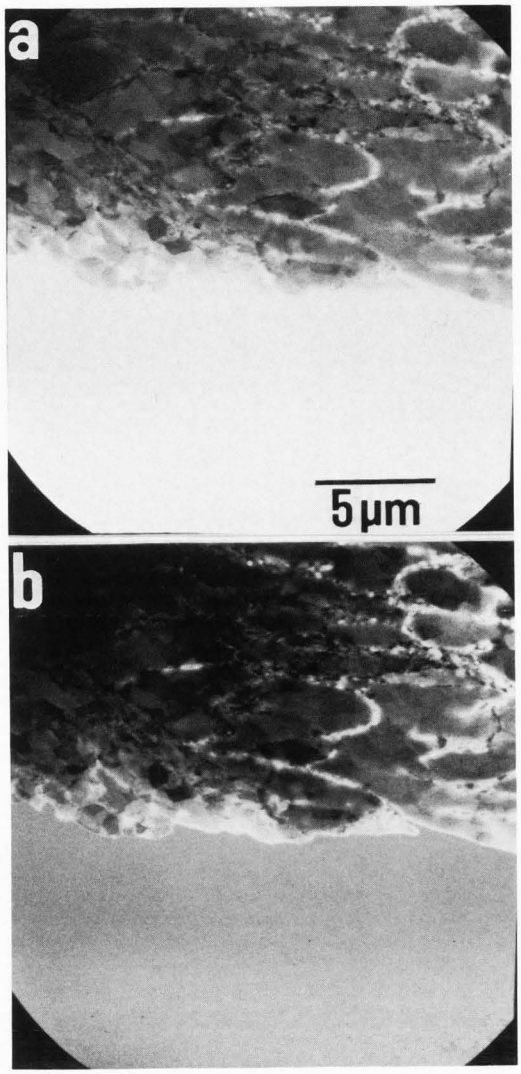

Fig. 12: a) TE and b) mixed TE/SE images taken of the edge of a sample of dynamically-compacted Al-6%Si powder particles. In a) the hole is the brightest object in the image; in b) the signal level of the hole has been reduced by mixing in the SE component. Note the improvement in contrast and image definition in the mixed image near the sample edge.

G.W. Bailey (ed), Claitor's Publishing, Baton Rouge, LA, 140-141.

Cliff G, Lorimer GW. (1972). Quantitative Analysis of Thin Metal Foils Using EMMA-4 - the Ratio Technique, in: Proceedings of the 5th European Congress on Electron Microscopy, Institute of Physics, London, 140-141.

Cliff G, Lorimer GW. (1975). The Quantitative Analysis of Thin Specimens. J. Microscopy 103, 203-207.

De Vries MI, Mastenbroek A. (1977). SEM Observations of Dislocation Substructures Around Fatigue Cracks in AISI Type 304 Stainless Steel. Metall. Trans. A 8A, 1497-1499.

Field DJ, Butler EP, Scamans GM. (1980). The Application of Electron Optical Techniques to the Study of Oxidation, in: Electron Microscopy and Analysis, 1979, T. Mulvey (ed), Institute of Physics, London, 401-404.

Field RD, Fraser HL. (1978). Microstructural Observations of Metal Powders Using Analytical Electron Microscopy. Metall. Trans. A 9A, 131-134.

Glitz RW, Notis MR, Williams DB, Goldstein JI. (1981). Considerations of X-ray Absorption for STEM X-ray Analysis of Ni-Al Foils, in: Microbeam Analysis 1981, R.H. Geiss (ed), San Francisco Press, San Francisco, 309-312.

Goldstein JI. (1975). Electron Optics, in: Practical Scanning Electron Microscopy, J.I. Goldstein, H. Yakowitz (eds), Plenum Press, New York, 21-48.

Goodhew PJ. (1972). Specimen Preparation in Materials Science, in: Practical Methods in Electron Microscopy, vol. 1, A.M. Glauert (ed), North-Holland Publishing, London, 1-180 (especially 128-134).

Hirsch PB, Partridge PG, Segall RL. (1959). An Electron Microscope Study of Stainless Steel Deformed in Fatigue and Simple Tension. Philos. Mag. 4, 721-729, Pl. 80-85.

Hosoi J, Inoue M, Kokubo Y, Hama K. (1981). Addition of Surface Information to STEM Image by Signal Processing. Scanning 4, 155-158.

Hren JJ. (1979). Specimen Contamination in Analytical Electron Microscopy: Sources and Solutions. Ultramicroscopy 3, 375-380.

Humphreys CJ. (1979). STEM Imaging of Crystals and Defects, in: Introduction to Analytical Electron Microscopy, J.J. Hren, J.I. Goldstein, D.C. Joy (eds), Plenum Press, New York, 305-332.

Isaacson M, Utlaut M, Kopf D. (1980). Analog Computer Processing of Scanning Transmission Electron Microscope Images, in: Computer Processing of Electron Microscope Images, P.W. Hawkes (ed), Springer-Verlag, New York, 257-283.

Johnson KA, Staudhammer KP, Reeves GA, Vesser LR. (1983). AEM/STEM Analysis of Vapor Deposited Multilayer Laser Targets, in: Microbeam Analysis 1983, R. Gooley (ed), San Francisco Press, San Francisco, 171-173.

Jones AV, Smith KCA. (1978). Image Processing for Scanning Microscopists. Scanning Electron Microsc. 1978; I: 13-26.

Katagiri K, Awatani J, Koyanagi K, Onishi Y, Tsuji M. (1980). Dislocation Structures Associated with Fracture Surface Topographies in Stage II Fatigue Crack Growth in Copper and 70:30 Brass. Metal Sci. 14, 485-492.

Kokubo Y, Inoue M, Hosoi J, Aita S. (1980). An Application of Secondary Electrons to STEM Imaging. Scanning 3, 285-288.

Lorimer GW, Cliff G, Clark JN. (1976). Determination of the Thickness and Spatial Resolution for the Quantitative Analysis of Thin Foils, in: Developments in Electron Microscopy and Analysis, J.A. Venables (ed), Academic Press, London, 153-156.

Loveluck JE, Rackham GM, Steeds JW. (1977). Electron Microscopy of Metal-Semiconductor Contacts, in: Developments in Electron Microscopy and Analysis 1977, D.L. Misell (ed), Institute of Physics, London, 297-300.

McConville RL. (1983). Improvements in the Electron Probe Forming Capabilities and X-ray Hole Counts in the Philips TEM, in: Proceedings of the 41st Annual Meeting EMSA, G.W. Bailey (ed), San Francisco Press, San Francisco, 376-377.

Nankivell JF. (1962a). Minimum Differences in Height Detectable in Electron Stereomicroscopy. Brit. J. Appl. Phys. 13, 126-128.

Nankivell JF. (1962b). Stereoscopic Viewing of Metal Foils in the Electron Microscope. Brit. J. Appl. Phys. 13, 129-130.

Newbury DE. (1975). Image Formation in the Scanning Electron Microscope, in: Practical Scanning Electron Microscopy, J.I. Goldstein, H. Yakowitz (eds), Plenum Press, New York, 95-148.

Nix KJ, Flower HM. (1982). The Metallography of Fatigue in the High-Strength Aluminium Alloy 7010, in: Advances in Fracture Research (Fracture '81), vol. 2, D. Francois (ed), Pergamon Press, New York, 915-922.

Osterlund R, Vingsbo O. (1978). Electron Microscopy on Etched Thin Foils: A Comparative SEM, STEM and TEM Analysis, in: Electron Microscopy 1978, vol. 1, J.M. Sturgess (ed), Microscopical Society of Canada, Toronto, 126-127.

Porter JR, Goldstein JI, Williams DB. (1979). Analytical Electron Microscopy of Electric Arc Furnace Dust, in: Proceedings of the 39th Annual Meeting EMSA, G.W. Bailey (ed), Claitor's Publishing, Baton Rouge, LA, 134-135.

Porter JR, Goldstein JI, Kim YW. (1982). Characterization of Directly Sampled Electric Arc Furnace Dust, in: Physics in the Steel Industry, F.C. Schwerer (ed), American Institute of Physics, New York, 377-393.

Rackham GM, Steeds JW. (1980). Nickel Germanium Gold Contacts to Gallium Arsenide, in: Electron Microscopy and Analysis 1979, T. Mulvey (ed), Institute of Physics, London, 157-160.

Scamans GM, Tuck CDS. (1979). Embrittlement of Aluminium Alloys Exposed to Water Vapour, in: Environment-Sensitive Fracture of Engineering Materials, Z.A. Foroulis (ed), TMS-AIME, Warrendale PA, 191-210.

Smith PJ, Wildman HS, Leighton A. (1979). Analysis of Al-Cu Corrosion by Analytical Electron Microscopy and Auger Spectroscopy, in: Proceedings of the 37th Annual Meeting EMSA, G.W. Bailey (ed), Claitor's Publishing, Baton Rouge, LA, 478-479.

von Heimendahl M, Willig V. (1980). A General Method for Determining Specimen Thickness. Norelco Reporter 27, 22-24.

Williams DB. (1982). Practical Electron Microscopy in Materials Science: Imaging Modes in the Analytical Electron Microscope...Chapter 3. Norelco Reporter 29, 28-41.

Williams DB, Edington JW. (1981a). Practical Electron Microscopy in Materials Science: Analytical Electron Microscopy. Norelco Reporter 28, 2-25.

Williams DB, Edington JW. (1981b). Practical Electron Microscopy in Materials Science: Alignment and Calibration of the AEM...Chapter 2. Norelco Reporter 28, 23-37.

Williams DB, Goldstein JI. (1981). Absorption Effects in Quantitative Thin Film X-ray Microanalysis, in: Analytical Electron Microscopy 1981, R.H. Geiss (ed), San Francisco Press, San Francisco, 39-46.

Zaluzec NJ. (1981). On the Geometry of the Absorption Correction for Analytical Electron Microscopy, in: Microbeam Analysis 1981, R.H. Geiss (ed), San Francisco Press, San Francisco, 325-328.

Discussion with Reviewers

D. B. Williams: Could you comment on the resolution in SE images in a STEM compared with similar images in a conventional SEM?
Author: The fact that the sample in a STEM is generally held within the objective lens of the microscope increases the resolution of SE images taken in a STEM. This is reflected in the resolution figures quoted by STEM and SEM manufacturers for SE images in their instruments. Several SEM manufacturers now allow for "high-resolution" modes of operation, which usually involve inserting small specimens up into the objective lenses of the instruments. Of course, forming an SE image with the sample located within the objective lens of an SEM requires such an instrument to have an SE detector located above the lens, as in a STEM.

E. L. Hall: Concerning the section describing the use of the SE imaging mode to set the proper overall sample geometry for STEM microanalysis, has the author compared results (for example, composition profiles) obtained with the sample oriented in the incorrect geometry versus the correct geometry? What is the magnitude of the error caused by this effect?
Author: An analysis similar to the one suggested has been carried out in a study of the absorption of Al K-alpha x-rays in an ion-milled foil of Ni-Al (Glitz, et al., 1981). Performing the analyses on this foil with the sample area in the "correct" and "incorrect" positions was found to introduce a factor of two error in the Ni K-alpha/Al K-alpha intensity ratio obtained for this strongly absorbing system. A means of correcting the usual absorption terms to take into account the wedge-shaped cross-section of a typical foil edge has been described elsewhere (Zaluzec, 1981).

L. E. Thomas: Many of the newer computer-based multichannel analyzer systems used for x-ray microanalysis offer capabilities for digital storage and color display of scanned images. What applications of mixed-mode STEM imaging do you envision for these systems?
Author: It is easy to imagine that the use of such a system to independently store a TE and an SE image from the same sample area, followed by later image processing and mixing of the stored images, could be quite useful in a variety of ways. Such a system would certainly be much more flexible than the analog system described in this paper. However, increasing the capabilities and flexibility of an image processing system also tends to increase the danger of introducing artifacts into the processed image which have no physical basis in the structure of the sample itself. As long as these advanced systems easily allow the user to compare processed images to the "raw" image components, such systems should certainly be of use for most of the applications described in this paper, particularly those in which backthinned samples are examined.

D. B. Williams: Given the obvious advantages of SE imaging in the STEM, why do you think there have been so few publications in the literature in which SE and combined SE/TE imaging are applied?
Author: Part of the reason lies in the fact that up until the advent of the latest generation of TEM/STEM instruments, the instrument manufacturers did not provide systems for easily comparing and mixing TE and SE images. Now that such systems are built in to the instruments by the manufacturers themselves, it seems likely that the use of SE and mixed TE/SE imaging in STEMs will pick up.

L. E. Thomas: For applications involving correlation of "top" and "bottom" surface images from thin specimens in a STEM, it may be worthwhile to modify the specimen holder so that it can be inverted in the microscope. Often this can be accomplished simply by changing the position of a locating pin on the holder. Also, the display can easily be rewired for image inversion to facilitate the comparison.
Author: Agreed.